Design of a Photoswitchable Cadherin

Ryan S. Ritterson,*[†,‡] Kristopher M. Kuchenbecker,[†] Michael Michalik,[‡,†] and Tanja Kortemme[†,‡]

[†]Graduate Group in Biophysics & [‡]California Institute for Quantitative Biomedical Research and Department of Bioengineering and Therapeutic Sciences, University of California, San Francisco, San Francisco, California 94158, United States

S *Supporting Information*

ABSTRACT: There is a growing interest in engineering proteins whose function can be controlled with the spatial and temporal precision of light. Here, we present a novel example of a functional light-triggered switch in the Ca-dependent cell−cell adhesion protein E-cadherin, created using a mechanism-based design strategy. We report an 18-fold change in apparent Ca^{2+} binding affinity upon illumination. Our results include a detailed examination of functional switching via linked changes in Ca^{2+} binding and cadherin dimerization. This design opens avenues toward controllable tools that could be applied to many long-standing questions about cadherin's biological function in cell−cell adhesion and downstream signaling.

There has been considerable interest in light-based control of biological systems,[1] and successful applications include light-modulation of neuronal ion channels,[2] light-switchable signaling proteins,[3] and light-controlled protein targeting.[4] Light-based methods offer titratable, precise spatial and temporal regulation that has been demonstrated *in vitro*,[5] in cell culture,[4,6] and in whole animals.[7] Most examples of light-based control fall into one of two categories: (a) those that are genetically encoded using a recombinantly produced protein borrowed from nature,[4] and (b) those created via targeted insertion of amino acids into a protein sequence and subsequent reaction with them of an exogenously introduced photoisomerizable small molecule, typically azobenzene based.[8] Azobenzene and related molecules undergo a reversible *cis−trans* isomerization when exposed to specific wavelengths of light, and this change in molecular shape can be coupled to changes in protein function. While in (a) the functional design is already provided naturally, one is limited both by the function (e.g., modulation of protein−protein binding, tuning fluorescence intensity) already encoded by the natural gene and by the requirement to fuse the natural protein with the protein to be modulated. In contrast, the designs in (b) allow many types of functional modulation, such as changes in agonist binding, protein−protein binding, and protein folding. In this work, we used a new strategy where changes in protein−ion affinity couple to protein dimerization, in the cell−cell adhesion protein cadherin (Figure 1A).

Cadherins are a key family of Ca-dependent cell−cell adhesion proteins and are divided into several subtypes, including the most commonly studied subtype, the classical cadherins. Classical cadherins, which include E-, N-, P-, R-, and C-cadherin,[9] are composed of an intracellular domain, a transmembrane helix, and five, repeated, extracellular domains labeled EC1 (N-terminal, membrane distal) to EC5 (C-terminal, membrane proximal),
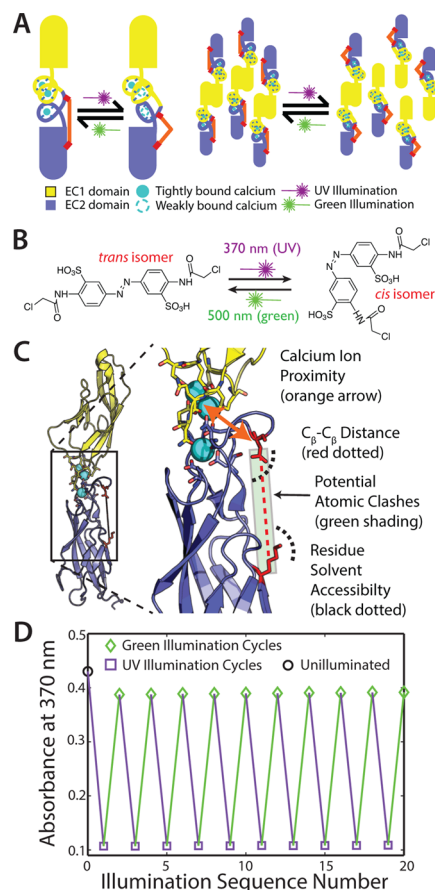

Figure 1. (A) A cartoon showing the basis of our design. As designed, our photoswitch reduces Ca^{2+} binding affinity, which, in turn, reduces homodimer affinity. (B) BSBCA undergoes a reversible cis/trans isomerization when illuminated with specific wavelengths of light. (C) EC12 structure showing the region targeted for photoswitchability. Labels indicate the design considerations. (D) Photoswitchability and reversibility measured by absorbance after many cycles of illumination of X-EC12.

along with three Ca^{2+} binding sites present in the loops at each extracellular domain boundary.[10,11] Calcium binding is required for cadherin function, as depletion of Ca^{2+} disrupts cadherin-mediated cell adhesion;[12] the presence of Ca^{2+} is suggested to rigidify the cadherin structure, allowing it to multimerize.[13] Knockdowns of cadherin significantly slow cell−cell adhesion,[14]

and in a classic experiment, cadherin-free, nonadherent cells transfected with cadherin acquire morphological similarities to naturally adherent cells.[15]

Our approach to creating a light-switchable cadherin aimed to modulate its Ca^{2+} binding affinity. Because Ca^{2+} binding is essential for cadherin multimerization, we reasoned that reversibly changing Ca^{2+} binding affinity would be an effective way to also modulate cadherin adhesive function (Figure 1A). We designed cysteine residues into the protein to serve as conjugation sites for an azobenzene-based photoisomerizable chromophore, BSBCA (Figure 1B). BSBCA has been used in previous applications,[5,16] demonstrating reversible switching between the *cis* and *trans* states when exposed to 370 nm (near UV) and 550 nm (green) light, respectively.[5] Our strategy involved conjugating both ends of the chromophore to the Ca-binding loops between cadherin domains EC1 and EC2, as these Ca^{2+} sites have previously been shown to be most critical for function.[11] In addition, because the Ca^{2+} binding sites are located in loop regions and bind Ca^{2+} with relatively weak affinities near 20 μM,[17] we reasoned it would be easier to induce conformational changes affecting Ca^{2+} binding there than in more rigid secondary structural elements or well-packed core regions of the protein.

Because BSBCA spontaneously cross-links cysteine residues,[18] the design challenge presented here can be generalized as the problem of finding the best pair of residues to mutate to cysteine. In practice, however, an enormous number of pairs are possible, the overwhelming majority of which are likely to be nonfunctional. We took a sequential and computational approach to identifying likely functional pairs (Figure S1 and Supporting Information [SI]). First, we used the program Rosetta[19] to computationally mutate all residues in four representative E-cadherin structures (PDB identifiers: 1FF5, 1EDH, 2O72, and 1Q1P) to alanine (the simplest mutation) and then calculated the predicted change in fold stability using a protocol we developed previously.[20,21] Residues with predicted destabilization >1 kcal/mol were not considered, as mutations to these residues were presumed to be disruptive. Next, we narrowed the pairs to those that would be geometrically compatible with the small molecule. We calculated pairwise C_β–C_β distances between the residues remaining using the 1FF5 structure and kept those pairs that fell in the range 17–20 Å (appropriate for the BSBCA *trans* isomer). Finally, the remaining pairs were ranked for an additional set of structural and geometric constraints (Figure 1C and SI). Eleven high-ranking pairs (Table S1) were cloned, expressed, and tested for conjugability (Figure S2), photoswitchability, and functionality (SI). One pair, K129C/D138C (Figure 1C, red residues) showed the best switchability and functionality, and was further characterized in detail.

We focused on, and expressed, the first two domains of E-cadherin (EC12), because they contain the homodimeric binding interfaces[22] and are the specificity determining domains,[23] making them most principally responsible for cadherin's function. Additionally, the shortened EC12 construct can be readily produced in high yields in *E. coli*. EC12 contains a single native cysteine residue, which we mutated to alanine (C9A), previously shown not to affect cadherin function.[24]

We first sought to show that K129C/D138C conjugated with *trans* BSBCA (termed X-EC12) could undergo isomerization to *cis*. Unconjugated BSBCA in the *trans* state has an absorbance peak near 370 nm that decreases when illuminated at this wavelength, resulting in a population that is 80–90% *cis*;

subsequent illumination at 500–550 nm will reverse the isomerization and produce a population that is >90% *trans*. Illuminating our conjugated protein (X-EC12) at 365 nm with a hand-held LED showed the characteristic reduction in absorbance of the *trans* state. The reverse isomerization (pan-visual illumination, including 500–550 nm bands) also behaved as expected, leading to a reappearance of the absorbance band of the *trans* state. We illuminated X-EC12 for 10 complete UV-green illumination cycles without any apparent loss of absorbance or switchability (Figure 1D); the switchability was also titratable via shorter illumination times (Figure S3).

We next tested whether isomerization changes Ca^{2+} binding affinity. To do so, we used a previously described mass spectrometry based assay[17] to directly measure the Ca^{2+} binding affinity of WT C9A as well as *trans* and *cis* X-EC12 (Figures 2A
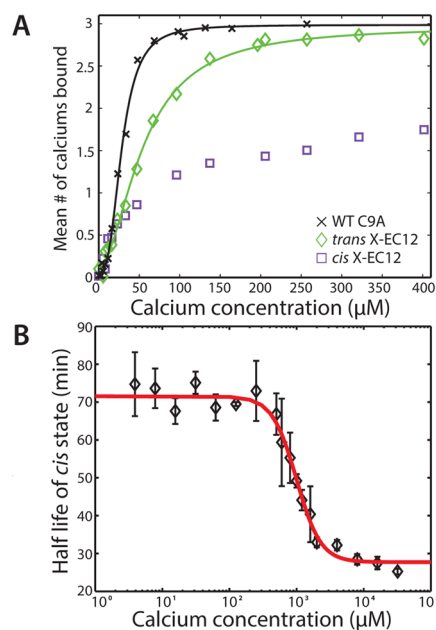

Figure 2. Characterization of photoswitchable Ca^{2+} binding affinity. (A) Ca^{2+} binding as monitored by mass spectrometry. While WT and *trans* X-EC12 bound three Ca^{2+} ions specifically, *cis* X-EC12 showed considerably weaker, predominantly nonspecific binding (Figure S4 and SI). Fits are based on a model of a single class of binding site for a maximum of three specifically bound Ca^{2+} ions. (B) The half-life of the *cis* state as a function of Ca^{2+} concentration, as measured by absorbance. Error bars are +1 SD from three independent experiments.

and S4; these assays used a cadherin concentration of 2 μM, significantly below a previously measured homodimeric K_d of WT cadherin (98.6 $\pm$ 15.5 μM),[22] to avoid potential complications due to cadherin dimerization). If isomerization alters Ca^{2+} binding, the *cis* X-EC12 should have weaker affinity than *trans*. In addition, because EC12 binds three Ca^{2+} ions, any of which could be interfered with, a decrease in apparent cooperativity as measured by the Hill coefficient (N_h) would be expected. WT C9A cadherin specifically bound three Ca^{2+} ions with a dissociation constant $K_d = 28.5 \pm 1.9$ μM (throughout the text, errors are the boundaries of a 95% confidence interval unless otherwise indicated) and extensive cooperativity with $N_h = 2.85 \pm 0.47$, close to previously reported numbers[17] of $K_d = 20 \pm 0.7$ μM and $N_h = 2.6 \pm 0.2$. *Trans* X-EC12 showed 2-fold weaker affinity and less cooperativity, with $K_d = 55.2 \pm 5.8$ μM and $N_h = 1.80 \pm 0.35$, but also bound three Ca^{2+} ions. In contrast, Ca^{2+} binding to *cis* X-EC12 was dominated by nonspecific binding. By

using quadruple and higher Ca-bound states from *trans* X-EC12 (Figure S5) as a reference for nonspecific binding, we subtracted the estimated contribution of nonspecific Ca^{2+} binding from the measured average Ca^{2+} occupancy for *cis* X-EC12 (SI). The resulting line shows significantly reduced binding compared to *trans*. (A quantitative fit was not possible due to required Ca^{2+} concentrations being higher than the dynamic range of the assay.)

To more directly measure the Ca^{2+} binding of *cis* X-EC12, we turned to a different assay that determined the *cis* half-life as a function of Ca^{2+} concentration. One general caveat inherant to azobenzene-based strategies is that switching to the *cis* state is generally incomplete; i.e., the *cis* state always contains a minor *trans* population.[8,18] However, the entirety of any change observed in half-life experiments is due only to the *cis* subpopulation, allowing measurement of pure *cis* properties unaffected by the small fraction that remains *trans*. Therefore, if chromophore isomerization significantly affects Ca^{2+} binding in our conjugated constructs, with stronger binding of Ca^{2+} to *trans* X-EC12, by thermodynamic coupling we would expect to see a change in the *cis* X-EC12 half-life with Ca^{2+} (Figure 2B). The *cis* state is thermodynamically unstable, and *cis* BSBCA relaxes back to the stable *trans* state in the dark with a half-life of ~20 min at 25 °C,[18] although conjugation to proteins can alter chromophore half-lives.[5,25] By observing the increase in absorbance at 370 nm during relaxation of our conjugated constructs back to *trans*, one can compute the half-life of the process (Figures S6 and S7; SI; these assays used a protein concentration of 12 μM to minimize potential changes in half-life due to protein dimerization). The half-life should decrease with increasing Ca^{2+} concentration as *trans* X-EC12 becomes stabilized by Ca^{2+} binding. As expected, we observed a half-life decrease from ~72 to 28 min, with an EC_{50} of 996 ± 135 μM Ca^{2+}. This represents a nearly 18-fold change in apparent Ca^{2+} binding affinity from the 55 μM for *trans* X-EC12 (mass spectrometry analysis, Figure 2A).

We also observed a cooperative transition in half-life duration, with a measured N_h of 2.4 ± 0.74. In showing interdependence between isomerization and Ca^{2+} binding, these results indicate that, as expected, isomerization of the chromophore significantly weakens Ca^{2+} binding. In addition, the observed cooperative nature indicates multiple Ca^{2+} ions are binding simultaneously during the transition from *cis* to *trans*, hinting that the *cis* state likely weakens multiple binding sites.

After successfully demonstrating photoswitchable Ca^{2+} binding in our engineered cadherin, we next asked whether the change in Ca^{2+} binding affinity also results in the expected change in protein binding activity. We used surface plasmon resonance (SPR) to measure protein homodimerization as a function of Ca^{2+} concentration (Figures 3, S8, and S9; SI). In this assay, similar to that of Harrison et al.,[22] biotinylated WT C9A cadherin was immobilized to the SPR chip and WT C9A, *trans* or *cis* X-EC12 were flowed over it. Direct measurements of both Ca^{2+} affinity and homodimeric protein affinity in SPR are difficult due to solution homodimers competing with those on the surface, reducing the effective protein concentration; to minimize solution homodimerization, we used a protein concentration (40 μM) below the K_d for homodimerization of WT EC12 cadherin.[22] Additionally, *cis* measurements are of mixed populations due to the inability of reaching full conversion to the *cis* state and some thermal relaxation to *trans* during the experiment, limiting the observable fold change in affinity (SI). We observed a Ca^{2+} binding EC_{50} for WT C9A cadherin, as measured by a single Hill fit, of 72.0 μM (with mean fit values and
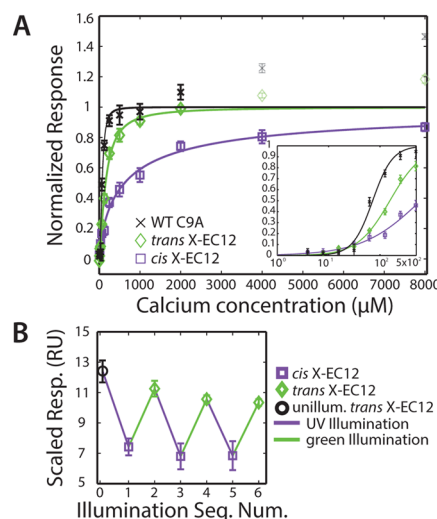

Figure 3. Characterization of photoswitch homodimeric binding. (A) Homodimeric binding monitored in SPR as a function of Ca^{2+} concentration. The data were fit to a Hill equation. Faded points contain significant nonspecific binding and were not used in the fits. Responses between flow cells were scaled to minimize a least-squares difference, and then mean values were normalized such that the fit value at $[Ca^{2+}] = \infty$ was 1.0 (SI). Error bars are ±1 SD of the three active flow cells in the instrument after scaling and normalization. Inset shows fits at low Ca^{2+} concentrations. (B) Homodimeric binding monitored in SPR at 1 mM Ca^{2+}, after repeated illumination cycles. Responses between flow cells were scaled to minimize a least-squares difference. Error bars are ±1 SD of the three active flow cells in the instrument after scaling.

±2 SD error, as measured by a bootstrapping analysis of the data, of 71.2 ± 14 μM; see SI and Figures S10, S11) and N_h = 2.24 (2.45 ± 1.7). In comparison, *trans* X-EC12 has an EC_{50} of 156 μM (170 ± 33 μM), with N_h = 1.38 (1.28 ± 0.28). These EC_{50} values are higher than those measured in the mass spectrometry assay (Figure 2A), which is due to cadherin binding multiple Ca^{2+} ions to function, causing any measured EC_{50} to necessarily be, at a minimum, a multiple of the protein concentration used, which here was 40 μM. Strikingly, *cis* X-EC12 showed substantially weakened binding (Figure 3A), with EC_{50} = 619 μM (611 ± 180 μM) and N_h = 0.76 (0.77 ± 0.15), demonstrating a nearly 4-fold change in Ca^{2+} affinity under these conditions. (Note: non-specific protein binding to the SPR chip appeared at Ca^{2+} concentrations >2 mM for WT C9A and *trans* X-EC12; see SI.) The change in protein−protein binding was also reversible as measured over multiple illumination cycles with 40 μM protein and 1 mM Ca^{2+} (Figure 3B).

An alternative explanation for the observed decrease in the SPR signal upon isomerization to the *cis* state could be an increase in *cis* homodimerization in solution, reducing the effective concentration of X-EC12 cadherin monomers available to bind to the WT cadherin immobilized on the chip. To exclude that possibility, we analyzed X-EC12 cadherin homodimerization via gel filtration. The observed decrease in the dimer/monomer ratio after UV illumination additionally confirms the expected weaker *cis* homodimerization upon illumination (Figure S12).

Questions remain about the structure of the functional cadherin multimers, including evidence that cadherin forms strand-swapped dimers.[22,26,27] While we cannot directly determine the structure of the interacting species formed in our SPR experiments, each set of SPR traces for a given cadherin variant can be fit to a single off rate returning to baseline levels, even at higher Ca^{2+} concentrations (Figure S13). This behavior is

consistent with a single dimer type formed for each assayed cadherin variant.

Taken together, our results demonstrate the successful design of a reversibly photoswitchable cadherin. When illuminated with light, its Ca^{2+} binding affinity changes from 56 to 996 μM, a nearly 18-fold change, and this change in affinity is coupled to a change in protein–protein binding. One constraint on our current design is the inability of BSBCA and other currently available chromophores to switch completely to *cis*. Several new chromophores have become available[25,28,29] that possess either more complete isomerization or longer half-lives that could allow for isolation and use of the pure *cis* state.

When applied in cell culture experiments, the light-modulatable cadherin could help answer several outstanding questions about cadherin's function. One way to introduce this engineered molecule into a cellular context is via cadherin-coated substrata. Coated substrata have been used to study cell–cell adhesion[30] and stem cell pluripotency.[31] Creation of coated surfaces allows spatial control of cadherin patterning and fine control over cadherin concentration, which could help maximize the switchability of cadherin-mediated adhesion.[30]

Although interest in photoswitchable proteins has increased in recent years, relatively few examples exist in the literature, perhaps because finding good cysteine attachment points remains difficult. Compared to high-throughput and other library techniques, we were able to create a successful conjugate using a rational design strategy and a small library of constructs. In our design, we chose to focus on modulating loop structures that may have a lower activation energy barrier to transition compared to more rigid parts of protein domains. While not all proteins could be modified in this way, we believe our combined rational/computational selection method and our focus on loops can be generalized to create other photoswitchable designs.

■ ASSOCIATED CONTENT

ⓢ Supporting Information

Data for other library members; detailed experimental methods; descriptions of, and figures for, data analysis methodology; additional figures for the unconjugated mutant. This material is available free of charge via the Internet at http://pubs.acs.org.

■ AUTHOR INFORMATION

Corresponding Author

ryan.ritterson@cal.berkeley.edu

Notes

The authors declare no competing financial interest.

■ ACKNOWLEDGMENTS

■ REFERENCES

(1) Krauss, U.; Drepper, T.; Jaeger, K. E. *Chemistry* **2011**, *17*, 2552.

(2) Banghart, M.; Borges, K.; Isacoff, E.; Trauner, D.; Kramer, R. H. *Nat. Neurosci.* **2004**, *7*, 1381.

(3) Wu, Y. I.; Frey, D.; Lungu, O. I.; Jaehrig, A.; Schlichting, I.; Kuhlman, B.; Hahn, K. M. *Nature* **2009**, *461*, 104.

(4) Levskaya, A.; Weiner, O. D.; Lim, W. A.; Voigt, C. A. *Nature* **2009**, *461*, 997.

(5) Woolley, G. A.; Jaikaran, A. S. I.; Berezovski, M.; Calarco, J. P.; Krylov, S. N.; Smart, O. S.; Kumita, J. R. *Biochemistry* **2006**, *45*, 6075.

(6) Zhang, F.; Muller, K. M.; Woolley, G. A.; Arndt, K. M. *Methods Mol. Biol.* **2012**, *813*, 195.

(7) Wyart, C.; del Bene, F.; Warp, E.; Scott, E. K.; Trauner, D.; Baier, H.; Isacoff, E. Y. *Nature* **2009**, *461*, 407.

(8) Beharry, A. A.; Woolley, G. A. *Chem. Soc. Rev.* **2011**, *40*, 4422.

(9) Ivanov, D. B.; Philippova, M. P.; Tkachuk, V. A. *Biokhimiya/ Biochemistry* **2001**, *66*, 1174.

(10) Koch, A.; Pokutta, S.; Lustig, A.; Engel, J. *Biochemistry* **1997**, *36*, 7697.

(11) Prakasam, A.; Chien, Y.; Maruthamuthu, V.; Leckband, D. *Biochemistry* **2006**, *45*, 6930.

(12) van Roy, F.; Berx, G. *Cell. Mol. Life Sci.* **2008**, *65*, 3756.

(13) Pokutta, S.; Herrenknecht, K.; Kemler, R.; Engel, J. *Eur. J. Biochem.* **1994**, *223*, 1019.

(14) Capaldo, C. T.; Macara, I. G. *Mol. Biol. Cell* **2007**, *18*, 189.

(15) Nose, A.; Nagafuchi, A.; Takeichi, M. *Cell* **1988**, *54*, 993.

(16) Guerrero, L.; Smart, O. S.; Woolley, G. A.; Allemann, R. K. *J. Am. Chem. Soc.* **2005**, *127*, 15624.

(17) Courjean, O.; Chevreux, G.; Perret, E.; Morel, A.; Sanglier, S.; Potier, N.; Engel, J.; van Dorsselaer, A.; Feracci, H. *Biochemistry* **2008**, *47*, 2339.

(18) Burns, D. C.; Zhang, F.; Woolley, G. A. *Nat. Protoc.* **2007**, *2*, 251.

(19) Rosetta - The premier software suite for macrommolecular modeling. http://www.rosettacommons.org (accessed May 16th 2013).

(20) Kortemme, T.; Baker, D. *Proc. Natl. Acad. Sci. U.S.A.* **2002**, *99*, 14116.

(21) Kortemme, T.; Kim, D.; Baker, D. *Sci. Signaling* **2004**, *2004*, l2.

(22) Harrison, O. J.; Bahna, F.; Katsamba, P. S.; Jin, X.; Brasch, J.; Vendome, J.; Ahlsen, G.; Carroll, K. J.; Price, S. R.; Honig, B.; Shapiro, L. *Nat. Struct. Mol. Biol.* **2010**, *17*, 348.

(23) Nose, A.; Tsuji, K.; Takeichi, M. *Cell* **1990**, *61*, 147.

(24) Troyanovsky, R. B.; Sokolov, E.; Troyanovsky, S. M. *Mol. Cell. Biol.* **2003**, *23*, 7965.

(25) Samanta, S.; Woolley, G. A. *ChemBioChem* **2011**, *12*, 1712.

(26) Troyanovsky, R. B.; Laur, O.; Troyanovsky, S. M. *Mol. Biol. Cell* **2007**, *18*, 4343.

(27) Häussinger, D.; Ahrens, T.; Aberle, T.; Engel, J.; Stetefeld, J.; Grzesiek, S. *EMBO J.* **2004**, *23*, 1699.

(28) Blanco-Lomas, M.; Samanta, S.; Campos, P. J.; Woolley, G. A.; Sampedro, D. *J. Am. Chem. Soc.* **2012**, *134*, 6960.

(29) Samanta, S.; Qin, C.; Lough, A. J.; Woolley, G. A. *Angew. Chem., Int. Ed.* **2012**, *51*, 6452.

(30) Borghi, N.; Lowndes, M.; Maruthamuthu, V.; Gardel, M. L.; Nelson, W. J. *Proc. Natl. Acad. Sci. U.S.A.* **2010**, *107*, 13324.

(31) Nagaoka, M.; Koshimizu, U.; Yuasa, S.; Hattori, F.; Chen, H.; Tanaka, T.; Okabe, M.; Fukuda, K.; Akaike, T. *PLoS ONE* **2006**, *1*, e15.